Electronic states of the DNA polynucleotides poly(dG)-poly(dC) in the presence of iodine

Masashi Furukawa and Hiroyuki S. Kato
RIKEN (The Institute of Physical and Chemical Research), Wako, Saitama 351-0198, Japan

Masateru Taniguchi and Tomoji Kawai
The Institute of Scientific and Industrial Research, Ibaraki, Osaka 567-0047, Japan

Takaki Hatsui and Nobuhiro Kosugi
UVSOR, Institute for Molecular Science, Myodaiji, Okazaki 444-8585, Japan

Tomoki Yoshida and Misako Aida
Center for Quantum Life Sciences and Department of Chemistry, Faculty of Science, Hiroshima University, Higashi-Hiroshima, Hiroshima 739-8526, Japan

Maki Kawai*
RIKEN (The Institute of Physical and Chemical Research), Wako, Saitama 351-0198, Japan
and Department of Advanced Materials Science, University of Tokyo, Kashiwa, Chiba 277-8651, Japan
(Received 21 April 2006; revised manuscript received 2 October 2006; published 19 January 2007)

The electronic states of chemically doped DNA polynucleotides [poly(dG)-poly(dC)] have been studied by photoelectron spectroscopy, x-ray absorption spectroscopy, and Raman spectroscopy, in order to understand the charge conduction mechanism of this material. Upon iodine doping (i.e., hole doping), we clearly observed radical cation formation on DNA bases, and the appearance of additional occupied and unoccupied electronic states within the band gap of poly(dG)-poly(dC). Referring to the analogous studies for π-conjugated conductive polymers, we point out that the charges induced by iodine doping and their derived electronic states are important origins of the hole-conductive electrical properties of poly(dG)-poly(dC).

DOI: 10.1103/PhysRevB.75.045119 PACS number(s): 71.20.Rv, 78.30.Jw, 79.60.Fr, 82.39.Pj

I. INTRODUCTION

Understanding the mechanism of charge conduction in DNA is of great importance not only for biochemistry but also for applications to molecular-scale electronic devices.[1–3] In the biochemical aspect, the charge conduction mechanism in DNA strands has been discussed for elucidation of long-range oxidative DNA damage and repair, in which hole migration has been examined mostly based on photoinduced charge transfer measurements using several types of modified DNAs in solutions[4–11] with various theoretical analyses.[12–18] Upon the progress in nanotechnology, from the end of the 1990s, the electric conductivity of DNA strands has directly been measured on a molecular scale under dry conditions,[20–26] which became a diverging point and provided us with the interesting subject of conductivity for one-dimensional organic molecules from the physical aspect.[1,3,27–35] Most of the above studies have claimed that the creation and stability of charges (particularly holes) are important for the charge conduction in DNA.

The charge conduction mechanism should reflect the electronic structure of the material. In the case of DNA, despite its importance, there are only limited numbers of experimental electronic state observations,[28,29,36] compared to the theoretical studies[18,19,23,31–33] to elucidate the charge conduction mechanism. From a physical point of view, therefore, we have investigated the electronic states of DNA (core levels, and occupied and unoccupied states around the Fermi level E_F) in the presence of hole charges. Since an oxidizing agent, such as iodine, creates hole charges in molecular materials, the iodine-doped DNA strands were prepared and characterized by means of several spectroscopic techniques under dry conditions.

In general, when holes are doped by chemical oxidation in an insulating neutral polymer, for example, polypyrrole and polythiophene, polymeric radical cation sites are created in it.[37–41] In doped polymers, simultaneously, localized occupied and unoccupied electronic states appear within the band gap, due to a local upward shift $\Delta\varepsilon$ of (the highest occupied molecular orbital (HOMO)) and a downward shift of (the lowest occupied molecular orbital (LUMO)).[38] These electronic states provide a high electrical conductivity, because the excitation energy of a hole from the additional occupied electronic states to the valence band decreases.[38] For these polymers, spectroscopic evidence confirming the doping effect is obtained, i.e., radical cation formation and appearance of new electronic states within the band gap. Radical ionic species can be detected from "chemical shifts" of core levels using x-ray photoelectron spectroscopy (x-ray PES).[42,43] The occupied and unoccupied electronic states near E_F can be obtained by vacuum-ultraviolet PES (vuv PES) and x-ray absorption spectroscopy (XAS), respectively.[43–46]

Taniguchi *et al.* have recently revealed that the dc conductivity of the homogeneous base-paired DNA polynucleotide poly(dG)-poly(dC) increases according to the rate of iodine doping (i.e., hole doping; oxidation), while another type of polynucleotide, poly(dA)-poly(dT), hardly shows such a characteristic feature.[7] This demonstrates that the hole charges are introduced into poly(dG)-poly(dC) upon iodine doping, similar to the case of π-conjugated conductive

polymers.[37–46] The aim of our present study is to experimentally characterize the iodine-doping effect on the electronic states of poly(dG)-poly(dC), and to clarify the origin of its electrical properties.

In this paper, we show the iodine-doping effect on the electronic and vibrational spectra of poly(dG)-poly(dC) using x-ray PES, vuv PES, XAS, and Raman spectroscopy. Quantum chemical simulations have also been carried out in order to support the Raman results. From PES and XAS, we confirmed the existence of radical cationic species on the DNA bases and the appearance of additional occupied and unoccupied electronic states within the intrinsic band gap of poly(dG)-poly(dC), when the iodine species were introduced into this material. The Raman spectra of iodine-doped poly(dG)-poly(dC) also showed evolution of the Raman band for the guanine radical cation, which allows us to conclude that the doping preferentially affects the guanine site and creates a hole in the poly(dG)-poly(dC) material.

II. EXPERIMENT

A. Spectroscopic measurements and quantum chemical simulations

PES and XAS measurements were performed at BL4B, UVSOR (IMS, Okazaki, Japan), in which the end station [ultrahigh vaccum (UHV)] is equipped with an electron energy analyzer (Scienta SES200) and a retarding-field electron detector for XAS.[28] The resolutions of x-ray PE spectra (Mg $K\alpha$, $h\nu$=1253.6 eV), vuv PE spectra ($h\nu$=170 eV), and N K-edge XA spectra were 1.0 eV, 150 meV, and 100 meV, respectively. Photon energies for XAS were calibrated using the energy separations of Au $4f_{7/2}$ peaks excited by the first-order (fundamental, $h\nu$) and second-order (false, $2h\nu$) diffraction lights of the grating.[28]

During PES measurements, an electron flood gun was used for all samples in order to exclude the charging effects. Binding energies (BE) for PESs were calibrated by referring to Si $2p$ of bulk p-type Si (99.1 eV),[47] and P $2p$ in the backbone of the DNA system. P $2p$ x-ray PE spectra always showed a singlet peak at BE of approximately 134.0 eV, with a full width at half maximum (FWHM) of 2.2–2.4 eV.[48]

Raman measurements were carried out under atmospheric conditions using a Jobin-Yvon U-1000 spectrometer (approximately 4 cm^{-1} resolution) at RIKEN (Wako, Japan). The excitation source was an Ar ion laser emitting at 514.5 nm (2.4 eV excitation). Since the notch filter was utilized for the reduction of excitation light in these measurements, the signals below 200 cm^{-1} was not obtained. At the spectra shown in this paper, a broad background component possibly due to luminescence was already subtracted. Vibration energies for the spectrometer were calibrated using that of toluene.[49]

In order to assign the Raman spectra, density functional theory calculations were carried out with the GAUSSIAN program[50] using Becke's three-parameter exchange functional in combination with the LYP correlation functional (B3LYP).[51] The 6-31G* basis set,[52,53] which is a split valence set and includes d polarization functions for heavy atoms, was used throughout this study as a compromise between accuracy and applicability to large molecules.

B. Sample preparation

The homogenous base-paired DNA double helix poly(dG)-poly(dC) (Amersham Biosciences, 1.7–2.9 μm long) was dissolved in deionized water (17.8 MΩ cm) at a concentration of 1.25 mg/ml, followed by dialyzation to reduce the concentration of sodium ions to approximately 10^3 ppm.[26] All the film samples were fabricated by casting this solution onto the substrates under atmospheric conditions. Depending on the measurement methods, suitable parameters such as substrates, film thickness, and doping time were selected as described below.

For PES and XAS measurements, we prepared poly(dG)-poly(dC) films (≈50 nm thick; Ref. 26) onto RCA-treated SiO_2/p-Si(111) substrates ($\rho \sim 10-50$ Ω cm).[54] The samples were mounted in a UHV chamber via a sample entry system from atmospheric conditions, without baking procedures.[28] Special care to maintain the freshness of the DNA samples was taken throughout the experiments, in order to avoid any chemical changes. In the PES and XAS experiments, the sample was frequently replaced with a new one, at least twice a day. This procedure also excluded the accumulation of x-ray radiation damage on the surface.[28]

Iodine-doped film samples were fabricated through exposure to iodine atmosphere of 10^{-5} Torr for 20 h at room temperature. According to Taniguchi *et al.*, the dc electrical conductivity reaches a maximum under these conditions, indicating that the dopant is saturated.[26] Since iodine is volatile, the actual amount of dopant was quantitatively analyzed for every sample, using x-ray PES, by integrating the photoelectron intensity of I $3d_{5/2}$ and comparing the relative intensity to that of N $1s$. In Sec. III A, the typical iodine-doping effects on the electronic states of poly(dG)-poly(dC) are discussed based on the PES and XAS results.

For Raman measurements, Al_2O_3(0001) was used as a substrate and thicker films of the order of micrometers were deposited; a thickness that is required for obtaining sufficient Raman signals. Iodine-doped samples were fabricated by exposing the film to iodine vapor of 10^{-5} Torr for almost 1 week at room temperature.[55] After the doping, samples were immediately transferred to the Raman spectrometer. The presence of dopant was also confirmed by the Raman bands arising from the vibration modes of anionic iodine species.[56,57] In Sec. III B, we show Raman spectra of iodine-doped poly(dG)-poly(dC) with various doping levels, and discuss the radical site strongly affected by the doping.

III. RESULTS

A. X-ray PES, vuv PES, and XAS

Figures 1(a)–1(c) show typical x-ray PE spectra (Mg $K\alpha$, $h\nu$=1253.6 eV) of nondoped and iodine-doped poly(dG)-poly(dC) films [substrate: SiO_2/p-Si(111); Ref. 54] in the region of the I $3d$ core levels. While the nondoped poly(dG)-poly(dC) film (hereafter NGC) does not show any I $3d$ photoemission signals [Fig. 1(a)], iodine-doped poly(dG)-

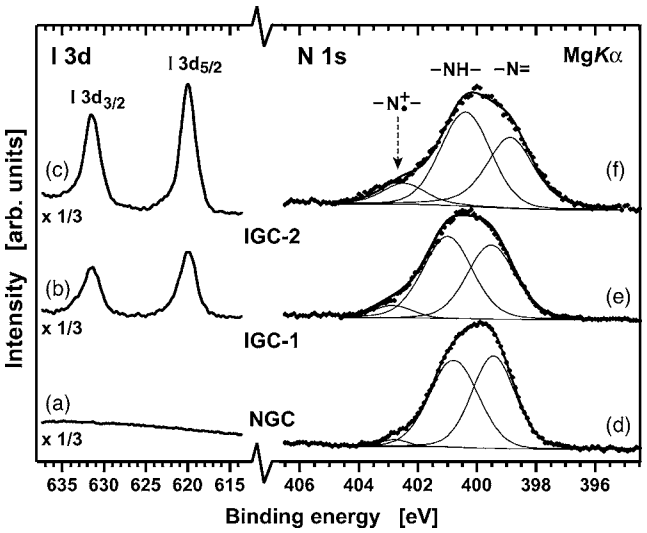

FIG. 1. X-ray PE spectra (Mg $K\alpha$, m $h\nu$=1253.6 eV) for nondoped poly(dG)-poly(dC) (NGC) and iodine-doped poly(dG)-poly(dC) (IGC-1 and IGC-2) films in the BE regions of (a)–(c) I 3*d* and (d)–(f) N 1*s* core levels. All of the film samples were fabricated onto SiO_2/p-Si(111) substrates with a thickness of approximately 50 nm. The measurements were done at room temperature with energy resolution of approximately 1.0 eV. For all of the displayed N 1*s* x-ray PE spectra, the raw data are plotted by closed diamonds. In the peak assignments for each N 1*s* spectrum, the contribution of secondary electrons was first subtracted from the raw data by means of the Proctor-Sherwood method. The individual N 1*s* components were evaluated by a least squares fitting. The iodine-doping effect is observed as the appearance of a higher-BE component attributed to the radical cationic nitrogen species.

poly(dC) films (hereafter IGC-1 and IGC-2) always provide doublet peaks at BEs of 620.0 and 631.1 eV, attributed to I $3d_{5/2}$ and I $3d_{3/2}$, respectively [Figs. 1(b) and 1(c)]. The observed BEs are identical to those for the iodine-doped C_{60} system,[58] and thus the iodine in IGC-1 and IGC-2 is identified to be the I_3^- ion, which implies that the evaporated iodine acts as an electron acceptor and may create holes in poly(dG)-poly(dC).[37]

Figures 1(d)–1(f) show N 1*s* core levels of NGC, IGC-1, and IGC-2. As described in the experimental section, the ratio of integrated photoelectron peak intensity of I $3d_{5/2}$ to that of N 1*s* provides the quantitative dopant concentration.[43] By considering the atomic sensitivity factors of I $3d_{5/2}$ and N 1*s* (4.4 and 0.38 at the Mg $K\alpha$ excitation, respectively),[48] we estimate the dopant concentration of IGC-1 to be 35%, which means that the ratio of the number of I_3^- ions to that of guanine-cytosine base pairs is approximately 1:3 in the observed region of IGC-1. The dopant concentration of IGC-2 is approximately 66%, which is almost twice as high as that of IGC-1. Comparing these two films at different doping levels, i.e., IGC-1 and IGC-2, with the nondoped sample (NGC), we characterized the effect of iodine doping on the chemical states of poly(dG)-poly(dC).

A typical effect of iodine doping appears as a chemical shift of N 1*s* core levels [Figs. 1(e) and 1(f)]. The N 1*s* for NGC consists of two main components [Fig. 1(d)]; one at around 401.0 eV and the other at around 399.5 eV, corresponding to the amine (—NH—) and imine (—N═) nitrogens, respectively.[59] For both of the doped samples IGC-1 and IGC-2 [Figs. 1(e) and 1(f)], the intensity of an additional photoelectron peak at higher BE region increases, which is attributed to a radical cationic nitrogen (—$N^+_\bullet$—: BE $\approx$402.8 eV). Simultaneously, the imine nitrogen peak decreases in its intensity. A small photoelectron peak attributed to the radical cationic nitrogen is recognized even for NGC [Fig. 1(d)], which probably is derived from the contribution of a small amount of initially oxidized species in poly(dG)-poly(dC).[42,60,61] In Table I, the composition of integrated intensities for imine, amine, and radical cationic nitrogen peaks to that of total N 1*s* is summarized. While the contribution of amine species is always the same ($\approx$50%), the imine species decreases and the radical cationic species increases with the increasing doping level. This suggests that imine species in guanine-cytosine base pairs are partially chemically transformed into a radical cationic species upon doping. Similar results have been reported for hole-doped polyaniline, a π-conjugated polymer containing imine nitrogen; Zeng *et al.*[42] and Nakajima *et al.*[62] have observed in x-ray PES measurements that a radical cation is formed at the nitrogen site of quinoid structural units when polyaniline was doped with iodine, HCl, and/or HBF_4.

The occupied electronic states near E_F for NGC, IGC-1, and IGC-2 were observed using vuv PES ($h\nu$=170 eV), as

TABLE I. Summary of the doping concentration of I_3^- ion and the relative composition of imine, amine, and radical cationic nitrogen atoms at three different film samples of nondoped poly(dG)-poly(dC) (NGC) and iodine-doped poly(dG)-poly(dC) (IGC-1 and IGC-2).

Sample	Doping concentration (%)[a]	Composition of each N 1*s* integral (%)[b]		
		—$N^+_\bullet$—	—NH—	—N═
IGC-2	65.582	10.841	48.960	40.204
IGC-1	34.955	5.659	50.730	43.610
NGC	0.000	2.233[c]	49.858	47.909

[a]Ratio of the number of I_3^- ions to that of guanine-cytosine base pairs by estimation from the I $3d_{5/2}$ and N 1*s* integral considering the atomic sensitivity factors (4.4 and 0.38 at Mg $K\alpha$ excitation, respectively).
[b]Composition estimated by fitting of the individual N 1*s* components, as shown in Fig. 1.
[c]This may be due to a small amount of initially oxidized species.

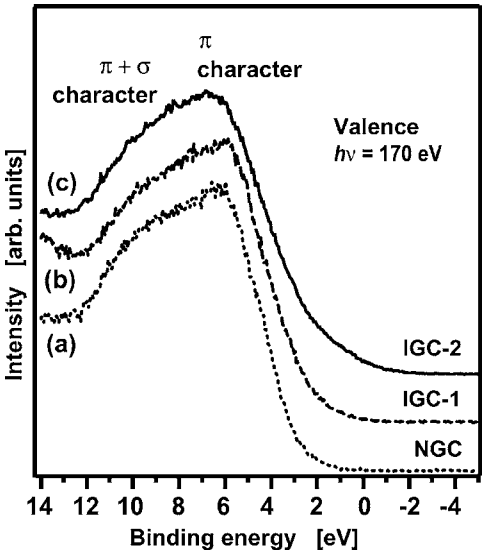

FIG. 2. Valence-band electronic states (occupied states) for (a) NGC (dotted line), (b) IGC-1 (dashed line), and (c) IGC-2 (solid line), characterized by vuv PES ($h\nu$=170 eV). These samples are the same ones utilized for the x-ray PES measurements shown in Fig. 1. The spectra were measured at room temperature with energy resolution of 150 meV. Overall the shapes of the spectra are comparable to each other, indicating that the chemical structure of poly(dG)-poly(dC) is not significantly modified upon iodine doping.

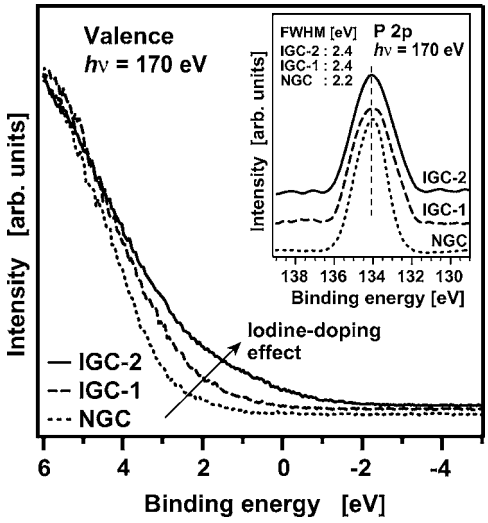

FIG. 3. Expanded VUV PE spectra in the range close to the valence band maximum for NGC (dotted line), IGC-1 (dashed line), and IGC-2 (solid line), in which the energy resolution is identical to that in Fig. 2. These samples are also the same ones utilized at the x-ray PES (Fig. 1) and VUV PES (Fig. 2) measurements. In the inset, P 2*p* core levels of these samples are displayed with their full width at half maximum values, which clearly indicate the broadening by charge-up or other effects was neglected in these measurements. The iodine-doping (hole-doping) effect is observed as a shift of the valence band edge toward the Fermi level (indicated by the arrow). This feature implies the appearance of additional occupied electronic states above the intrinsic π band of poly(dG)-poly(dC).

shown in Fig. 2. Two major intense bands are detected at around 6 and 10 eV. These binding energies resemble those reported for π-conjugated polymers,[63] where they are assigned to the energy for the orbitals with π character and $\pi+\sigma$ character, respectively. These spectra show that the general shapes of spectra are basically the same, which indicates that the chemical structure of poly(dG)-poly(dC) is not significantly modified upon iodine doping.[43]

A prominent effect caused by the iodine doping is observed close to the valence band maximum (Fig. 3). As the doping level increases (IGC-1 and IGC-2), the onset of spectrum gradually shifts toward E_F, compared with that for NGC. Core level spectra of P 2*p* are also shown in the inset of this figure, where an identical single peak centered at around 134.0 eV is observed with the FWHM value of 2.2–2.4 eV.[48] Since these values do not significantly differ from each other, the observed shifts in the valence band edge do not reflect the broadening of the spectra due to charge-up or other effects, which is often suffered as a problem in PES measurements for organic materials. We conclude that the observed shift in the valence band edge is due to a change in the valence state, i.e., the appearance of new occupied electronic states above the intrinsic π band, which is caused by the modification of occupied electronic states of poly(dG)-poly(dC) upon iodine doping. This is basically in good agreement with the features observed for π-conjugated conductive polymers.[43,44] For example, Bätz *et al.* have investigated the valence band electronic states of polypyrrole films and have found that anion doping (i.e., hole doping) causes a shift of the peak edge relative to its E_F, indicating a *p*-type electrical conductivity.[43]

The unoccupied electronic states of NGC, IGC-1, and IGC-2 were observed by XAS of the N *K*-edge, as shown in Fig. 4. The N *K*-edge spectrum for NGC [Fig. 4(a)] shows three characteristic resonance peaks, which resembles those reported by Kirtley *et al.* previously.[36] They are attributed to the excitation from N 1*s* core levels to $\pi^*_{-N=}$ (photon en-

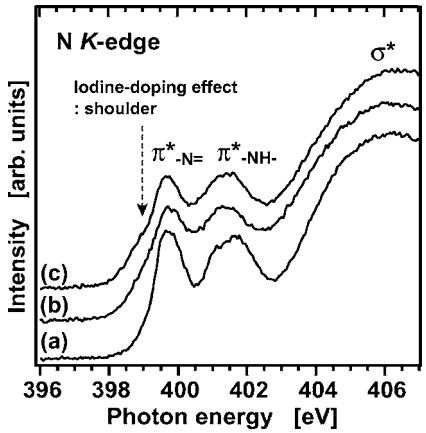

FIG. 4. Unoccupied electronic states for (a) NGC, (b) IGC-1, and (c) IGC-2 characterized by nitrogen *K*-edge XAS. These samples are the same ones utilized in Figs. 1–3. The spectra were measured at room temperature with a resolution of 300 meV, and the intensities were normalized in the regions of 395–398 and 420–425 eV (not shown here). A typical iodine-doping (hole-doping) effect is observed as the appearance of a shoulder component below the $\pi^*_{-N=}$ resonance peak (indicated by the arrow). This feature implies the appearance of additional unoccupied electronic states below the intrinsic π^* band of poly(dG)-poly(dC).

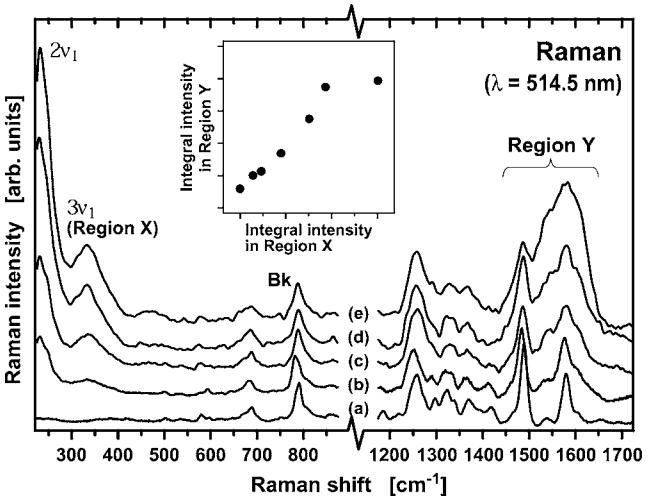

FIG. 5. Raman spectra (Ar ion laser excitation, $\lambda=514.5$ nm) of (a) nondoped poly(dG)-poly(dC), and (b)–(e) iodine-doped poly(dG)-poly(dC) at various doping levels. For these measurements, the films were fabricated onto $Al_2O_3(0001)$ substrates with a thickness of the order of micrometers. The measurements were carried out under atmospheric conditions with a resolution of approximately 4 cm^{-1}. Intensities of the obtained spectra were normalized with the Raman peak at 788 cm^{-1} (O-P-O stretch vibration mode in the backbone of the DNA strand, denoted "Bk"). The $2\nu_1$ and $3\nu_1$ ("Region *X*") Raman bands correspond to the second and third harmonics of the symmetrical stretching mode of the I_3^- ion, respectively ($\nu_1 \approx 107$ cm^{-1}). The Raman band of "Region *Y*" is mainly contributed by the deformation mode of guanine (partly, that of cytosine). The inset plots the Raman intensity integral of Region *Y* versus that of Region *X*. From this relationship, it is clear that the evolution of the Region *Y* Raman band strongly depends on the amount of I_3^- ion in the sample.

ergy of 399–401 eV), π^*_{-NH-} (401–404 eV), and σ^* (above 405 eV) states.[36,64] For iodine-doped samples of IGC-1 and IGC-2 [Figs. 4(b) and 4(c), respectively], the absence of shifts in the continuum σ^* resonance suggests that the bond lengths, and thus the π-conjugated ring structure, do not change markedly upon doping,[45] which are also confirmed in the vuv PE spectra, as mentioned above in the text and the captions of Fig. 2.

The effect of iodine doping appears in the $\pi^*_{-N=}$ resonance peak. The intensity of $\pi^*_{-N=}$ resonance peak height is reduced slightly, accompanied by the appearance of a shoulder in the low-energy side [Figs. 4(b) and 4(c)]. Referring to the XAS studies of π-conjugated conductive polymers,[45,46] we conclude that the iodine doping provides the appearance of new unoccupied states below the intrinsic π^* band of poly(dG)-poly(dC).

Consequently, from x-ray PES, vuv PES, and XAS, we have found two distinct features, when the I_3^- ions are introduced into this material: the radical cation formation on DNA bases (Fig. 1), and the appearance of additional occupied and unoccupied electronic states within the intrinsic band gap of poly(dG)-poly(dC) (Figs. 2–4). In the next section, we show the results of Raman spectra in order to reveal the most chemically affected site of this material upon doping.

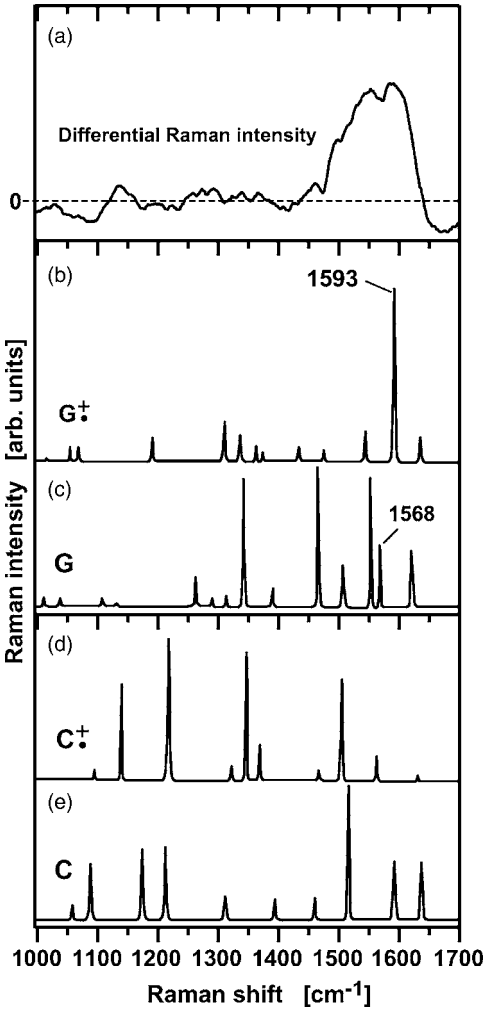

FIG. 6. (a) Difference in Raman intensities between nondoped and iodine-doped poly(dG)-poly(dC) spectra [Figs. 5(a) and 5(e), respectively]. The signal change originating from the iodine doping is clearly seen in the higher-wave-number regions. Calculated Raman spectra (B3LYP/6-31G*) are shown for (b) radical cation phase of guanine ($G^+_.$), (c) neutral guanine (G), (d) radical cation phase of cytosine ($C^+_.$), and (e) neutral cytosine (C). A scale factor of 0.96 was used for the calculated vibration frequencies.

B. Raman spectroscopy

Typical Raman spectra of iodine-doped and nondoped poly(dG)-poly(dC) films (substrate: $Al_2O_3(0001)$), taken with Ar ion laser excitation ($\lambda=514.5$ nm; 2.4 eV), are displayed in Fig. 5. Raman shifts for nondoped poly(dG)-poly(dC) [Fig. 5(a)] are assigned as follows according to the literature:[65–69] Two peaks at 1259 and 1546 cm^{-1} are attributed to the deformation modes (deformations) of cytosine. The peaks at 1329, 1365, 1485, 1579, and 1602 cm^{-1} are the deformations of guanine, and 1417 cm^{-1} is the $C(2')H_2$ scissor mode in the deoxyribose. The peak at 788 cm^{-1} is the O–P–O stretching mode in the backbone ("Bk" in this figure).[69] As a whole, the shape of this spectrum indicates that this material is a mixture of *A*- and *B*-formed double helices.[69]

In the Raman spectra of iodine-doped poly(dG)-poly(dC) [Figs. 5(b)–5(e)], the effect of iodine doping appear in the

regions of $\nu < 400$ cm^{-1} and $1450 < \nu < 1650$ cm^{-1}. Two Raman bands, observed below 400 cm^{-1}, are attributed to the second and third harmonics of the symmetric stretching mode ($\nu_1 \approx 107$ cm^{-1}) of I_3^-, i.e., $2\nu_1$ and $3\nu_1$ ("Region *X*" in this figure), respectively.[56,57] Although the ν_1 band cannot be detected directly because the notch filter cuts off the light below ~ 200 cm^{-1}, the observed $2\nu_1$ and $3\nu_1$ bands clearly indicate again that iodine is in the form of I_3^- ion in iodine-doped poly(dG)-poly(dC), as described in the previous section [see the I 3*d* levels characterized with x-ray PES; Figs. 1(b) and 1(c)]. Note that the intensities of these $2\nu_1$ and $3\nu_1$ bands decreased gradually during the measurements, which is due to the volatility of iodine under our conditions of Raman measurements. Consequently, Raman spectra of different amount of I_3^- dopant were obtained [Figs. 5(b)–5(e)], which allows us to discuss the doping effect on the Raman signals of iodine-doped poly(dG)-poly(dC) under various doping levels, as described below.

As the Raman signals of $2\nu_1$ and $3\nu_1$ (Region *X*) increase in intensity, the evolution of a Raman band in region of $1450 < \nu < 1650$ cm^{-1} (Region *Y*) increases. Comparing these spectra with that of nondoped poly(dG)-poly(dC) [Fig. 5(a)], the Raman band in the region of $1450 < \nu < 1650$ cm^{-1} (mainly deformations of guanine), rather than that in $1200 < \nu < 1300$ cm^{-1} (deformations of cytosine), shows broadening and enhancement with increasing the doping level. This feature is also confirmed in the inset of Fig. 5, where the integrated intensity of Region *Y* is almost proportional to that of Region *X*.

The spectrum evolution due to iodine doping is more clearly exhibited in the difference spectrum between nondoped and iodine-doped poly(dG)-poly(dC) [Figs. 5(a) and 5(e), respectively], as shown in Fig. 6(a). In order to understand the origin of this difference spectrum, Raman spectra were theoretically calculated (B3LYP/6-31G*) for single guanine and cytosine molecules with their neutral and radical cationic phases [Figs. 6(b)–6(e)]. The spectrum of a guanine radical cation [$G_{\cdot}^+$; Fig. 6(b)] shows a characteristic peak at 1593 cm^{-1} that is at least four times larger than the other peaks, whereas that of cytosine radical cation [$C_{\cdot}^+$; Fig. 6(d)] shows four peaks in the region of 1100–1500 cm^{-1}. The intense peak at 1593 cm^{-1} of $G_{\cdot}^+$ [Fig. 6(b)] originates from the enhancement and the blueshift of the peak at 1568 cm^{-1} of neutral guanine [G; Fig. 6(c)], which is attributed mainly to the stretching vibration of C(3)-N(4).[68] These results indicate that the difference spectrum [Fig. 6(a)] reflects the theoretical spectrum of $G_{\cdot}^+$ [Fig. 6(b)] rather than $C_{\cdot}^+$ [Fig. 6(d)], which means that the radical cation formation [as observed also in the x-ray PES of N 1*s*; Figs. 1(e) and 1(f)] preferentially occurs at the guanine site in poly(dG)-poly(dC) upon iodine doping (hole doping). The $G_{\cdot}^+$ formation is quite reasonable from the experimental and theoretical studies on the oxidation of nucleobases.[60,61]

IV. DISCUSSION

A. Charge conduction upon iodine doping

According to the current-voltage measurements performed by Taniguchi *et al.*, the electric conductance of nondoped poly(dG)-poly(dC) is quite low, i.e., insulating.[26] The results from visible-ultraviolet absorption spectroscopy and theoretical simulations also show that the material intrinsically has the band gap of a few eV.[18,33,70] The electrical conductivity of DNA strands is increased by chemical doping with iodine,[26] as well as the hole doping by electric field.[25] Based on those measurements, it was expected that the iodine doping would create hole charges in poly(dG)-poly(dC) and thus increase the conductivity.

As investigated from our spectroscopic study, iodine exists as an I_3^- ion [Figs. 1(a)–1(c)] interacting with poly(dG)-poly(dC). As a result, the iodine doping provides hole charges and creates $G_{\cdot}^+$ species (Figs. 1, 5, and 6). We have also found the appearance of additional occupied and unoccupied electronic states within the intrinsic band gap of the material upon doping (Figs. 2 and 3). Since the features observed in the electrical conductivity measurement[26] and our spectroscopic results resemble those of π-conjugated conductive polymers,[42–46] we conclude that the charges induced by doping and their derived electronic states play significant role in the electrical properties of hole-doped poly(dG)-poly(dC).[25,26] This implies that the enhancement of electrical conductivity is due to a decrease in the excitation energy of a hole from the additional occupied electronic states to the valence band.[38]

In order to further explain the charge conduction process in this material, we have to mention two antithetical models.[22] One is bandlike conduction, in which the injected charge is instantaneously delocalized through a continuous molecular orbital of DNA strand. Another one is charge hopping, in which the charge hops between the discrete (localized) molecular orbital of adjacent base pairs. A similar matter has already been discussed for distance dependence of hole migration rate at photoinduced charge transfer measurements of DNA in solutions.[4–16] Consequently, it is generally accepted that the hole hopping between DNA base orbirals is dominant for the long-range charge migration, while the ballistic tunneling process is effective for short transfer, by the results of experimental[11] and theoretical[12–16] studies. In electric conductivity studies in molecular scale, this matter must be discussed again because of the various experimental reports explained using the delocalized electronic states[21,22,24,34] and the localized electronic states.[20,23,25,28,30–33,35]

Our experimental results, especially from Raman measurement, have revealed that the doped hole charge is localized on guanine (Figs. 5 and 6), but not on cytosine, deoxyribose, or phosphate. Our finding is in good agreement with the theoretical report given by Alexandre *et al.*,[31] where *ab initio* calculations for both neutral and hole-doped fragments of poly(dG)-poly(dC) with one to four guanine-cytosine base pair(s) are carried out. Their calculation results have shown that the HOMO of hole-doped poly(dG)-poly(dC) is spreaded mostly on a single guanine base, but not on cytosine; in the other words, a hole charge is confined to a single guanine base. They have also suggested that the lengths of hydrogen bonds between guanine and cytosine are modified a little upon doping, which leads to a hole-lattice coupling interaction.[31]

The localization of a hole charge would also be expected from the electronic states of nondoped

poly(dG)-poly(dC).[28,33] For example, the lifetime of resonantly excited π^* states (LUMO) from the N 1*s* core state was found to be longer than several femtoseconds, which corresponds to the core hole lifetime (the time scale of Auger transition).[28] This means that the LUMO of poly(dG)-poly(dC) consists of localized molecular orbital. Since its HOMO is energetically deeper and more compact in shape, it should be more localized compared to LUMO. The band calculations given by Taniguchi *et al.* have suggested that the transfer integral between guanine's HOMO in poly(dG)-poly(dC) is small and thus the bandwidth at the valence band is narrow.[33] Therefore, the hole charge most likely tends to localize on each guanine. Consequently, it is natural to consider charge-hopping conduction, rather than bandlike conduction, as the origin of charge conduction in poly(dG)-poly(dC), where the charge hops between the adjacent base pairs, overcoming some activation barrier E_a. According to the experiments on *I-V* characteristics for poly(dG)-poly(dC), the E_a value for the hole hopping has been estimated to be 0.12 eV at around room temperature,[25] which is in agreement with the theoretically estimated hopping activation energy of 0.15 eV.[31] However, the exact argument of the hopping rate derived from the electronic states should take account of additional factors at a finite temperature, such as practical phonon coupling,[10,35] reorganization and free energies,[12,16] and counterion effects,[18,32] as discussed so far.

B. Created states at $G_{\cdot}^{+}$

In this section, we focus on the created electronic states in iodine-doped poly(dG)-poly(dC), in connection with the enhanced Raman signals of $G_{\cdot}^{+}$ species in Figs. 5 and 6 (Sec. III B). As described in Secs. III B and IV A, we conclude that the iodine doping affects the guanine site in poly(dG)-poly(dC) and creates the radical cationic species, i.e., $G_{\cdot}^{+}$. Our results also hold the possibility that the signal arising from $G_{\cdot}^{+}$ species was observed strongly due to a resonance enhancement effect[37] by the $G_{\cdot}^{+}$-derived electronic states, for which the absorption should occur at 514.5 nm (2.4 eV) excitation (Ar ion laser utilized in our Raman measurement), as follows.

In a study of pulse radiolysis measurements,[71,72] it has been shown that the radical cationic phase of deoxyguanosine and 1-methylguanosine, and short-length DNA oligonucleotides containing $G_{\cdot}^{+}$ have a broad absorbance band, which is continuously located in the visible-light region of $\lambda = 450-700$ nm (i.e., 1.7–2.8 eV), in which the maximum absorption is located at $\lambda_{max} \approx 460-480$ nm (2.6–2.7 eV). This "broad" band appears in addition to an intrinsic π-π^* absorption band ($\lambda_{max} \approx 260$ nm; 4.8 eV).[70] Therefore, our sample, iodine-doped poly(dG)-poly(dC) containing $G_{\cdot}^{+}$, is also considered to have a similar absorption band in this visible-light region. This feature is actually expected from our vuv PES and XAS results (Figs. 2–4), in which the additional occupied and unoccupied electronic states appear above the intrinsic π band and below the intrinsic π^* band of poly(dG)-poly(dC), respectively.

Because of the electronic features discussed above, it is expected that our Raman result reveals a direct relationship between the new electronic states (Figs. 2–4) and radical cation formed on guanine (Figs. 1, 5, and 6). With the 514.5 nm (2.4 eV) excitation, a resonance Raman effect may have occurred, in which the vibration signal arising from $G_{\cdot}^{+}$ species (Figs. 1, 5, and 6) was observed obviously due to the excitation of their derived electronic states (Figs. 2–4). Resonance Raman spectroscopy for π-conjugated conductive polymer systems has been summarized by Furukawa,[37] where the enhancement is explained by the existence of charged self-localized excitations, such as polarons.[38] In terms of polymer science, a positive polaron (hole polaron) is regarded as a sort of radical cation associated with a lattice distortion and with the presence of two localized states within the band gap, i.e., an occupied (half-filled) polaron state and an unoccupied (empty) polaron state.[37,38] Our findings of the radical cation and the additional occupied and unoccupied states within the intrinsic band gap for iodine-doped poly(dG)-poly(dC) are in good agreement with the general polaron electronic states.

For the charge conduction mechanism of DNA, the polaronic behavior has already been suggested from photoinduced charge transfer measurement,[10] current-voltage characteristics,[25] and theoretical calculations.[17,30,31,35] For example, Yoo *et al.* have suggested, from their current-voltage characteristic measurements, that the temperature-dependent electrical conductivity is explained by a polaron hopping model.[25] In addition, as described in the previous section, the theoretical calculation given by Alexandre *et al.* have shown that the hole doping provides a modification of lengths of hydrogen bond between guanine and cytosine, which leads to a hole-lattice coupling interaction, causing a small polaron.[31] Together with the above studies, our findings by several spectroscopic characterizations additionally give evidence for the existence of a polaron state in hole-doped poly(dG)-poly(dC). Since polaronlike conduction of the DNA strands has been proposed in both solution[10,17] and dry[25,30,31,35] conditions, our results seem to be reflecting a common electronic feature for the charge conduction mechanism in DNA.

Finally, it is noted that the 514.5 nm (2.4 eV) excitation may also contribute to the light absorption of the I_3^- ion ($\lambda_{max} \approx 440$ nm; 2.8 eV).[70] Therefore, the observed large Raman signals of $2\nu_1$ and $3\nu_1$ (the second and third harmonics of the stretch vibration of the I_3^- ion; ν_1) in Fig. 5 have probably been enhanced by the resonant excitation.

V. CONCLUSIONS

We have investigated the hole-doping effect on the electronic states of iodine-doped poly(dG)-poly(dC), in order to understand the possible electrical conduction mechanism in this material. When iodine was introduced into this material, x-ray PE spectra and Raman spectra have identified the chemical structure of dopant species to be the I_3^- ion. Upon iodine doping, we found the appearance of additional occupied and unoccupied electronic states within the band gap and the radical cation species formed favorably at the guanine site, i.e., $G_{\cdot}^{+}$. These electronic state features are analogous to π-conjugated conducting polymers, where their

electrical conductivities are enhanced due to the doping. Therefore, we conclude that the positive charges, i.e., holes, induced by iodine doping induce additional electronic states which will play an essential role in the charge conducting properties of poly(dG)-poly(dC) DNA.

ACKNOWLEDGMENTS

We express our appreciation to T. Tahara, S. Shin, T. Komeda, M. Trenary, S. Yamaguchi, T. Takeuchi, H. Oji, and M. Tamura for valuable discussions and technical support. M.F. appreciates the Special Postdoctoral Researchers Program of RIKEN. This work was supported by the Joint Studies Program of IMS, the 21st Century Center of Excellence (COE) program under the Ministry of Education, Culture, Sports, Science and Technology of Japan, and the RIKEN Research Programs "Nanoscale Science and Technology Research" and "Molecular Ensemble Research."

*Corresponding author. Email address: maki@riken.jp

[1] *Long-Range Charge Transfer in DNA I and II*, edited by G. B. Schuster (Springer-Verlag, Berlin, 2004), and references therein.
[2] R. G. Endres, D. L. Cox, and R. R. P. Singh, Rev. Mod. Phys. **76**, 195 (2004), and references therein.
[3] M. Taniguchi and T. Kawai, Physica E (Amsterdam) **33**, 1 (2006), and references therein.
[4] A. M. Brun and A. Harriman, J. Am. Chem. Soc. **114**, 3656 (1992).
[5] C. J. Murphy, M. R. Arkin, Y. Jenkins, N. D. Ghatlia, S. H. Bossmann, N. J. Turro, and J. K. Barton, Science **262**, 1025 (1993).
[6] S. Priyadarshy, S. M. Risser, and D. N. Beratan, J. Phys. Chem. **100**, 17678 (1996).
[7] F. D. Lewis, T. Wu, Y. Zhang, R. L Letsinger, S. R. Greenfield, and M. R. Wasielewski, Science **277**, 673 (1997).
[8] K. Fukui and K. Tanaga, Angew. Chem., Int. Ed. **37**, 158 (1998).
[9] C. Wan, T. Fiebig, S. O. Kelley, C. R. Treadway, J. K. Barton, and A. H. Zewail, Proc. Natl. Acad. Sci. U.S.A. **96**, 6014 (1999).
[10] P. T. Henderson, D. Jones, G. Hampikian, Y. Kan, and G. B. Schuster, Proc. Natl. Acad. Sci. U.S.A. **96**, 8353 (1999).
[11] B. Giese, J. Amaudrut, A.-K. Köhler, M. Spormann, and S. Wessely, Nature (London) **412**, 318 (2001).
[12] A. Okada, V. Chernyak, and S. Mukamel, J. Phys. Chem. A **102**, 1241 (1998).
[13] J. Jortner, M. Bixon, T. Langenbacher, and M. E. Michel-Beyerle, Proc. Natl. Acad. Sci. U.S.A. **95**, 12759 (1998).
[14] M. Ratner, Nature (London) **397**, 480 (1999).
[15] F. C. Grozema, Y. A. Berlin, and L. D. A. Siebbeles, J. Am. Chem. Soc. **122**, 10903 (2000).
[16] H. L. Tavernier and M. D. Fayer, J. Phys. Chem. B **104**, 11541 (2000).
[17] S. V. Rakhmanova and E. M. Conwell, J. Phys. Chem. B **105**, 2056 (2001).
[18] F. L. Gervasio, P. Carloni, and M. Parrinello, Phys. Rev. Lett. **89**, 108102 (2002).
[19] J. P. Lewis, T. E. Cheatham, III, E. B. Starikov, H. Wang, and O. F. Sankey, J. Phys. Chem. B **107**, 2581 (2003).
[20] E. Braun, Y. Eichen, U. Sivan, and G. Ben-Yoseph, Nature (London) **391**, 775 (1998).
[21] H.-W. Fink and C. Schönenberger, Nature (London) **398**, 407 (1999).
[22] D. Porath, A. Bezryadin, S. de Vries, and C. Dekker, Nature (London) **403**, 635 (2000).
[23] P. J. de Pablo, F. Moreno-Herrero, J. Colchero, J. Gomez Herrero, P. Herrero, A. M. Baró, P. Ordejón, J. M. Soler, and E. Artacho, Phys. Rev. Lett. **85**, 4992 (2000).
[24] A. Y. Kasumov, M. Kociak, S. Guéron, B. Reulet, V. T. Volkov, D. V. Klinov, and H. Bouchiat, Science **291**, 280 (2001).
[25] K.-H. Yoo, D. H. Ha, J.-O. Lee, J. W. Park, J. Kim, J. J. Kim, H.-Y. Lee, T. Kawai, and H. Y. Choi, Phys. Rev. Lett. **87**, 198102 (2001).
[26] M. Taniguchi, H.-Y. Lee, H. Tanaka, and T. Kawai, Jpn. J. Appl. Phys., Part 2 **42**, L215 (2003).
[27] Z. Kutnjak, C. Filipic, R. Podgornik, L. Nordenskiöld, and N. Korolev, Phys. Rev. Lett. **90**, 098101 (2003).
[28] H. S. Kato, M. Furukawa, M. Kawai, M. Taniguchi, T. Kawai, T. Hatsui, and N. Kosugi, Phys. Rev. Lett. **93**, 086403 (2004).
[29] H. Wadati, K. Okazaki, Y. Niimi, A. Fujimori, H. Tabata, J. Pikus, and J. P. Lewis, Appl. Phys. Lett. **86**, 023901 (2005).
[30] Y. Asai, J. Phys. Chem. B **107**, 4647 (2003).
[31] S. S. Alexandre, E. Artacho, J. M. Soler, and H. Chacham, Phys. Rev. Lett. **91**, 108105 (2003).
[32] H. Kino, M. Tateno, M. Boero, J. A. Torres, T. Ohno, K. Terakura, and H. Fukuyama, J. Phys. Soc. Jpn. **73**, 2089 (2004).
[33] M. Taniguchi and T. Kawai, Phys. Rev. E **70**, 011913 (2004).
[34] R. A. Caetano and P. A. Schulz, Phys. Rev. Lett. **95**, 126601 (2005).
[35] M. Taniguchi and T. Kawai, Phys. Rev. E **72**, 061909 (2005).
[36] S. M. Kirtley, O. C. Mullins, J. Chen, J. van Elp, S. J. George, C. T. Chen, T. O'Halloran, and S. P. Cramer, Biochim. Biophys. Acta **1132**, 770 (1992).
[37] Y. Furukawa, J. Phys. Chem. **100**, 15644 (1996).
[38] J. L. Brédas and G. B. Street, Acc. Chem. Res. **18**, 309 (1985).
[39] A. J. Heeger, S. Kivelson, J. R. Schurieffer, and W.-P. Su, Rev. Mod. Phys. **60**, 781 (1988).
[40] J. L. Brédas, J. C. Scott, K. Yakushi, and G. B. Street, Phys. Rev. B **30**, 1023 (1984).
[41] A. J. Epstein, J. M. Ginder, F. Zuo, R. W. Bigelow, H.-S. Woo, D. B. Tanner, A. F. Richter, W.-S. Huang, and A. G. MacDiarmid, Synth. Met. **18**, 303 (1987).
[42] X.-R. Zeng and T.-M. Ko, J. Polym. Sci., Part B: Polym. Phys. **35**, 1993 (1997).
[43] P. Bätz, D. Schmeisser, and W. Göpel, Phys. Rev. B **43**, 9178 (1991).
[44] G. Tourillon and Y. Jurget, J. Chem. Phys. **89**, 1905 (1988).
[45] A. P. Hitchcock, G. Tourillon, R. Garnett, and N. Lazarz, J. Phys. Chem. **93**, 7624 (1989).
[46] G. Appel, G. Böhme, R. Mikalo, and D. Schmeißer, Chem. Phys. Lett. **313**, 411 (1999).
[47] *Handbook of X-Ray Photoelectron Spectroscopy*, edited by G. E.

Muilenberg (Perkin-Elmer, MN, 1978).
[48] H. Shigekawa, H. Ikawa, R. Yoshizaki, Y. Iijima, J. Sumaoka, and M. Komiyama, Appl. Phys. Lett. **68**, 1433 (1996).
[49] *Raman Bunkou-Hou*, edited by H. Hamaguchi and A. Hirakawa (Gakkai-shuppan Center, Tokyo, 1998) (in Japanese).
[50] Computer code GAUSSIAN 98, revision A.11.3, Gaussian, Inc., Pittsburgh PA, 2002.
[51] A. D. Becke, J. Chem. Phys. **98**, 5648 (1993).
[52] P. C. Hariharan and J. A. Pople, Chem. Phys. Lett. **16**, 217 (1972)
[53] W. J. Hehre, R. Ditchfield, and J. A. Pople, J. Chem. Phys. **56**, 2257 (1972).
[54] T. Yasuda, Y. Ma, Y. L. Chen, G. Lucovsky, and D. Maher, J. Vac. Sci. Technol. A **11**, 945 (1993).
[55] The time required for full doping is essentially related to the diffusion rate of iodine onto/into the GC films. Since the films for Raman measurements were much thicker than those for PES and XAS measurements, the time for doping had to be increased.
[56] W.-T. Chen, G. A. Bowmaker, J. M. Seakins, and R. P. Cooney, Appl. Spectrosc. **56**, 909 (2002).
[57] I. Harada, Y. Furukawa, M. Tasumi, H. Shirakawa, and H. Ikeda, J. Chem. Phys. **73**, 4746 (1980).
[58] H. Werner, M. Wesemann, and R. Schlogl, Europhys. Lett. **20**, 107 (1992).
[59] L. S. Shlyakhtenko, A. A. Gall, J. J. Weimer, D. D. Hawn, and Y. L. Lyubchenko, Biophys. J. **77**, 568 (1999), and references therein.
[60] Y. Yoshioka, Y. Kitagawa, Y. Takano, K. Yamaguchi, T. Nakamura, and I. Saito, J. Am. Chem. Soc. **121**, 8712 (1999).
[61] C. J. Burrows and J. G. Muller, Chem. Rev. (Washington, D.C.) **98**, 1109 (1998), and references therein.
[62] T. Nakajima, M. Harada, R. Osawa, T. Kawagoe, Y. Furukawa, and I. Harada, Macromolecules **22**, 2644 (1989).
[63] H. Sakamoto, M. Itow, N. Kachi, T. Kawahara, K. Mizoguchi, H. Ishii, T. Miyahara, K. Yoshioka, S. Masubuchi, S. Kazama, T. Matsushita, A. Sekiyama, and S. Suga, J. Electron Spectrosc. Relat. Phenom. **92**, 159 (1998).
[64] M. Furukawa, H. Fujisawa, S. Katano, H. Ogasawara, Y. Kim, T. Komeda, A. Nilsson, and M. Kawai, Surf. Sci. **532-535**, 261 (2003).
[65] E. W. Small and W. L. Peticolas, Biopolymers **10**, 69 (1971).
[66] E. W. Small and W. L. Peticolas, Biopolymers **10**, 1377 (1971).
[67] H. Dong, V. A. Bloomfield, J. M. Benevides, and G. J. Thomas, Jr., Biopolymers **50**, 656 (1999).
[68] M. Majoube, Ph. Milliè, P. Lagant, and G. Vergoten, J. Raman Spectrosc. **25**, 821 (1994).
[69] Y. Nishimura, C. Torigoe, and M. Tsuboi, Nucleic Acids Res. **14**, 2737 (1986).
[70] The Chemical Society of Japan (Ed.): *Kagaku-Binran Kiso-hen* 3rd ed. (Chemical Society of Japan, Tokyo, 1984), p. II-593 (in Japanese).
[71] L. P. Candeias and S. Steenken, J. Am. Chem. Soc. **111**, 1094 (1989).
[72] K. Kobayashi and S. Tagawa, J. Am. Chem. Soc. **125**, 10213 (2003).